TIME AND FREQUENCY DOMAIN ANALYSIS OF MARINE STRUCTURES IN SHORT-CRESTED SEA BY SIMULATING APPROPRIATE NODAL LOADS

C. Georgiadis
SINTEF, The Foundation of Scientific and Industrial Research
Norwegian Institute of Technology
Trondheim, Norway

ABSTRACT

This paper deals with the evaluation of the response of marine structures in short-crested sea states when the load spatial-correlation is an important factor. A commonly method of approach is using the frequency domain solutions of stochastic dynamics, by implementing the statistical properties of the loading in the cross spectral matrices. A simpler approach which can be used for time or frequency domain analysis is presented in this paper. A set of nodal forces is simulated, via a Monte Carlo simulation, fullfilling the statistical properties and the spatial-correlation of the applied loading, and the dynamic response is evaluated like a deterministic analysis. The solution is repeated for a number of different simulated nodal force sets, and the expected response values are obtained by computing ensemble statistics. The proposed method can be easily implemented in dynamic analysis finite element programs without significant needs of computation time and computer memory.

INTRODUCTION

In the case of marine structures in a short-crested wave field there exist mostly statistical information, like spectral densities and correlation functions, about the loading. The time histories of the loading cannot be predicted for each point of the structure. For the correct evaluation of the dynamic response, using a finite element model of the structure, one needs realistic nodal forces.

The usual method in stochastic dynamics (1) for calculating the response is frequency domain analysis, in which the frequency response function is evaluated for a number of unit harmonic waves at various frequencies and directions, and where the cross spectral load matrix is constructed from the directional wave spectrum and the hydrodynamic force functions.

In this paper a different approach is presented. The sea state is not decomposed in directional components, but it is represented by the wave coherence in various directions, and the hydrodynamic force functions are modified to include the directional effects. From the short crested sea state, using a Monte Carlo simulation, nodal loads are simulated, and are used in the finite element model for a deterministic dynamic analysis. The expected response values are obtained from ensemble statistics between the calculated response values in a number of simulated nodal load sets.

The proposed in this paper method can be used for time or frequency domain analysis. In the time domain analysis, constant values are assumed for the hydrodynamic force functions and the wave coherence, which is a fair approximation for narrow-banded wave loading.

The computer implementation of the proposed method is easy for any dynamic analysis finite element program, for frequency or time domain analysis, without significant needs in computation time and computer memory. Examples of using the method in the case of steel jacket and gravity offshore platforms and long floating structures are shown. Numerical results and comparison with field measurments are shown for a floating bridge under short-crested wave loading.

MATHEMATICAL STATEMENT OF THE PROBLEM

In a finite element formulation the structural response is

$$\mathbf{M_s}\ddot{\mathbf{d}} + \mathbf{C_s}\dot{\mathbf{d}} + \mathbf{K}\,\mathbf{d} = \mathbf{Q} \quad , \tag{1}$$

where: $\mathbf{d}$ is the vector of time dependent nodal displacements; $\mathbf{M_s}$, $\mathbf{C_s}$ and $\mathbf{K}$ are mass, damping and stiffness matrices of the structure-soil system; $\mathbf{Q}$ is the vector of time dependent hydrodynamic forces.

Depending on the size of the structural element the hydrodynamic forces are computed using Morison's equation or wave diffraction theory (2,3). Assuming linearizartion in the drag forces, and grouping terms depending on the structure motion on the left side and terms depending on the wave characteristics on the right side, Eq.(1) becomes

$$(\mathbf{M_s} + \mathbf{M_h} + \mathbf{C_m})\ddot{\mathbf{d}} + (\mathbf{C_s} + \mathbf{C_h} + \mathbf{C_d})\dot{\mathbf{d}} + \mathbf{K}\mathbf{d} = \mathbf{F_I} + \mathbf{F_d} + \mathbf{F_h} \quad , \tag{2}$$

where: $\mathbf{M_h}$ and $\mathbf{C_h}$ are the matrices of hydrodynamic mass

and damping due to waves generated by the structure obtained from potential theory; $\mathbf{C_m}$ and $\mathbf{C_d}$ are the inertia and drag contributions obtained from the linearized Morison's equation; $\mathbf{F_i}$ and $\mathbf{F_d}$ are inertia and drag forces obtained from Morison's equation and depend on the water particle acceleration and velocity; $\mathbf{F_h}$ is the vector of hydrodynamic forces on an immovable structure obtained from potential theory.

This paper shows a method to simulate the right hand vectors of Eq.(2) from the characteristics of the short-crested wave field. A time or frequency domain solution of Eq.(2) can be performed afterwards. The stochastic characteristics of the sea state are introduced by obtaining a set of solutions for different simulated cases and getting the ensemble statistics of the results.

Throughout this paper linear wave theory is assumed, also linearized Morison's equation and linear transformation from wave amplitude to wave forces. For the time domain analysis a narrow banded wave loading process is assumed so the hydrodynamic force coefficients and wave coherence are constant values. For simplicity most of the equations will be obtained by a time domain analysis, thus the hydrodynamic force functions and wave coherence will appear to be frequency independent. The frequency dependence of the final equations for the frequency domain analysis will be reintroduced, and the narrow-banded wave loading assumption is not necessary in the frequency domain analysis.

SHORT-CRESTED WAVE LOADING

Consider a coordinate system as the one shown in Fig.(1), where r(x,y,z) is used for the position vector of a point, and u(x,y) for the position of its projection on the free surface.

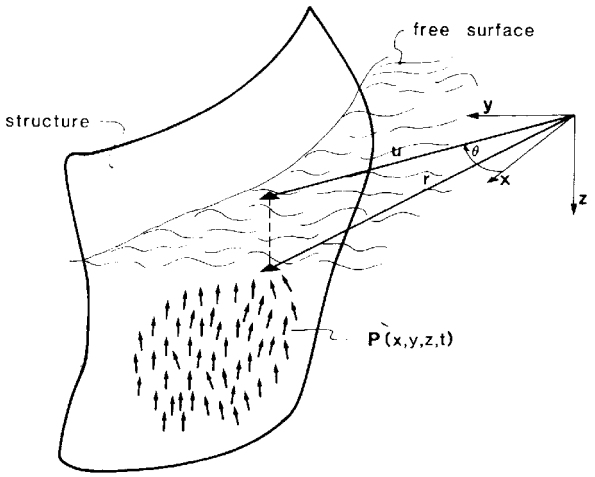

FIG. 1 GEOMETRICAL DEFINITIONS

We assume that the short-crested wave field is described by the directional wave spectrum (4)

$$S_W(\omega,\theta) = S_W(\omega)\ \Psi(\theta) \quad , \tag{3}$$

where $S_W(\omega)$ is the unidirectional spectrum (models like Pierson-Moskwitz, JONSWAP); and $\Psi(\theta)$ is a spreading function giving the directional distribution of the wave energy (5,6,7) (models like $\Psi(\theta)=C\cos^n(\theta-\theta_0)$, $\Psi(\theta)=C\cos^{2n}(\frac{\theta-\theta_0}{2})$, θ_0 is the mean wave direction).

For the directional wave spectrum the wave coherence $\gamma(\mathbf{u}_1,\mathbf{u}_2,\omega)$ between two points on the sea surface can be obtained (8). As the statistical properties of the wave field do not vary from point to point, the wave coherence depends on the vector separation ($\Delta\mathbf{u}=\mathbf{u}_1-\mathbf{u}_2$) between the two points

$$\gamma(\frac{\Delta\mathbf{u}}{\lambda}) = \sqrt{\left\{\left[\int_{-\pi/2+\theta_0}^{\pi/2+\theta_0}\Psi(\theta)\cos(2\pi(\frac{\Delta x}{\lambda})\cos\theta+2\pi(\frac{\Delta y}{\lambda})\sin\theta)\,d\theta\right]^2 + \left[\int_{-\pi/2+\theta_0}^{\pi/2+\theta_0}\Psi(\theta)\sin(2\pi(\frac{\Delta x}{\lambda})\cos\theta+2\pi(\frac{\Delta y}{\lambda})\sin\theta)\,d\theta\right]^2\right\}} \quad , \tag{4}$$

where λ is the wave length (for deep waters $\lambda=2\pi g/\omega^2$), and θ_0 is the mean wave direction. In ref.(9) graphs are presented for the above coherence of various directional spectral models. The wave coherence is a decaying function as the separation of the two points increases and can be approximated reasonably by an exponentialy decaying function (9,10,11,12). Tables for the coefficients of such exponential approximation are presented in refs.(8) and (12).

The surface waves create a time varying distributed load on the surface of the structure. For a surface element dS this load is

$$\mathbf{p}(\mathbf{r},t)dS = \begin{Bmatrix} p^x(x,y,z,t) \\ p^y(x,y,z,t) \\ p^z(x,y,z,t) \end{Bmatrix} dS \quad . \tag{5}$$

Depending on the size of the structural element two different approaches are used to compute the wave loading (2,13,14), Morison's equation and diffraction theory.

For slender members Morison's equation gives

$$\mathbf{p}(\mathbf{r},t)dS = \mathbf{C_i}\dot{\mathbf{v}} + \mathbf{C_d}\,\mathbf{v}\,|\mathbf{v}| \quad , \tag{6}$$

where $\mathbf{v}$ and $\dot{\mathbf{v}}$ is the normal water particle velocity and acceleration. Using linearized form of Eq.(6) we have

$$\mathbf{p}(\mathbf{r},t)dS = \mathbf{C_i}\dot{\mathbf{v}} + \mathbf{C_d}\sqrt{(8/\pi)}\,\sigma_v\,\mathbf{v} \quad . \tag{7}$$

For large members the diffraction theory gives

$$\mathbf{p}(\mathbf{r},t)dS = \mathbf{C_f}\ \eta(\mathbf{u},t) \quad , \tag{8}$$

where $\mathbf{C_f}$ is the frequency depended hydrodynamic coefficient, and $\eta(\mathbf{u},t)$ is the wave amplitude.

For harmonic wave loading of frequency ω and direction θ_0, $\mathbf{v}$ and $\dot{\mathbf{v}}$ in Eq.(7) are related linearly to the wave amplitude and both Eq.(7) and (8) can be expressed in the form

$$\mathbf{p}(\mathbf{r},t) = \begin{Bmatrix} \delta^x(\mathbf{r},\omega,\theta) \\ \delta^y(\mathbf{r},\omega,\theta) \\ \delta^z(\mathbf{r},\omega,\theta) \end{Bmatrix} \eta(\mathbf{u},t) \quad , \tag{9}$$

where $\delta(\mathbf{r},\omega,\theta)$ are the hydrodynamic force coefficients.

In this work the effect of the short-crested wave field is considered directly in the response calculations, without assuming a superposition of directional components. In this case the hydrodynamic coefficients of Eq.(9) should be modified to represent the directional spread of the wave energy. This can be done (12,15) if we use the spectral form of Eq.(9), and define the hydrodynamic force coefficients in the directional wave field as

$$\bar{\delta}(\mathbf{r},\omega,\theta_0) = \sqrt{\int_{-\pi/2+\theta_0}^{\pi/2+\theta_0}\delta^2(\mathbf{r},\omega,\theta)\Psi(\theta)\,d\theta} \quad . \tag{10}$$

The wave force on an element dS is

$$\mathbf{p}(\mathbf{r},t)dS = \eta(\mathbf{u},t)\ \mathbf{H}(\mathbf{r},\omega,\theta_0)\ dS \quad , \tag{11}$$

where $\mathbf{H}(\mathbf{r},\omega,\theta_0)$ is the hydrodynamic transfer function

$$\mathbf{H}(\mathbf{r},\omega,\ \theta_0) = \begin{Bmatrix} \bar{\delta}^x(\mathbf{r},\omega,\theta_0) \\ \bar{\delta}^y(\mathbf{r},\omega,\theta_0) \\ \bar{\delta}^z(\mathbf{r},\omega,\theta_0) \end{Bmatrix} \quad . \tag{12}$$

The mean wave direction is considered constant through all the analysis so the parameter θ_0 is taken out of the expression of the hydrodynamic transfer function. The hydrodynamic transfer function is frequency dependent, but in the following discussion because some equations will appear in time domain and some in frequency domain the hydrodynamic transfer function will be written as $\mathbf{H}(\mathbf{r})$, and will be assumed constant in the time domain analysis and frequency dependent in the frequency domain analysis. The constant values of the hydrodynamic and coherence functions in the time domain analysis is a fair aproximation for the case of narrow-banded wave loading.

The load correlation between two points $\mathbf{r}_1(x_1,y_1,z_1)$ and $\mathbf{r}_2(x_2,y_2,z_2,)$ of the structure surface is computed using Eq.(11) as

$$\mathbf{R}_p(\mathbf{r}_1,\mathbf{r}_2,\tau) = \begin{bmatrix} R_p^{xx} & R_p^{xy} & R_p^{xz} \\ R_p^{yx} & R_p^{yy} & R_p^{yz} \\ R_p^{zx} & R_p^{zy} & R_p^{zz} \end{bmatrix} = \lim_{T\to\infty} \frac{1}{T} \int_0^T \mathbf{p}(\mathbf{r}_1,t)\ \mathbf{p}^T(\mathbf{r}_2,t+\tau)dt$$

$$= \mathbf{H}(\mathbf{r}_1)\ \mathbf{H}^T(\mathbf{r}_2)\ R_\eta(u_1,u_2,\tau) \quad , \tag{13}$$

where $R_\eta(u_1,u_2,\tau)$ is the wave correlation between the projections u_1 and u_2 of the two points on the sea surface.

The load cross spectral matrix is obtained as the Fourier transform of the load correlation

$$\mathbf{S}_p(\mathbf{r}_1,\mathbf{r}_2,\omega) = \frac{1}{2\pi} \int_{-\infty}^{\infty} \mathbf{R}_p(\mathbf{r}_1,\mathbf{r}_2,\tau)\ e^{-i\omega\tau} d\tau$$

$$= \mathbf{H}(\mathbf{r}_1)\ \mathbf{H}^T(\mathbf{r}_2)\ S_\eta(u_1,u_2,\omega) \quad , \tag{14}$$

where $S_\eta(u_1,u_2,\omega)$ is the wave cross spectral matrix between the points u_1 and u_2 on the surface. Introducing the wave coherence in Eq.(14), we obtain for the amplitude of the load cross spectral matrix

$$|\mathbf{S}_p(\mathbf{r}_1,\mathbf{r}_2,\omega)| = \mathbf{H}(\mathbf{r}_1)\ \mathbf{H}^T(\mathbf{r}_2)\ \gamma(\Delta\mathbf{u},\omega) S_W(\omega) \quad . \tag{15}$$

FINITE ELEMENT MODEL

In a finite element model of the structure, with displacement formulation (16), the displacements inside an element (i,j,k,...) (Fig.2), are expressed as

$$\mathbf{q}(\mathbf{r}) = \begin{Bmatrix} q_x^x(\mathbf{r}) \\ q_y^y(\mathbf{r}) \\ q_z^z(\mathbf{r}) \end{Bmatrix} = \left[\mathbf{N}_i^e, \mathbf{N}_j^e, \ldots\right] \begin{Bmatrix} \mathbf{d}_i \\ \mathbf{d}_j \\ \vdots \end{Bmatrix}^e = \mathbf{N}^e\ \mathbf{d}^e \quad , \tag{16}$$

where $\mathbf{N} = N_i^e \mathbf{I}$; N_i^e are the element shape functions; $\mathbf{I}$ is a (3*3) identity matrix taking care of the three coordinate directions x,y,z; and $\mathbf{d}_i = [d_i^x, d_i^y, d_i^z]^T$ are the nodal displacements of node i. The superscript e designates that the corresponding matrices containing all the submatrices for a particular element e.

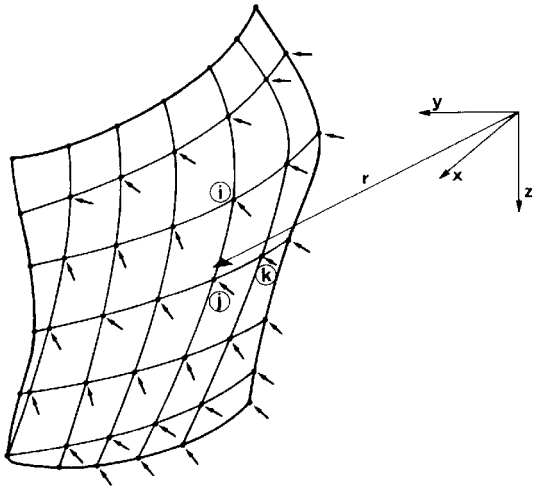

FIG.2 FINITE ELEMENT MODEL

After a variational formulation of the finite element equations, the nodal loads are expressed as

$$\bar{\mathbf{F}}(t) = \begin{Bmatrix} \mathbf{F}_1(t) \\ \mathbf{F}_2(t) \\ \vdots \end{Bmatrix} = \int_S \mathbf{N}^T \mathbf{p}(\mathbf{r},t) dS \quad , \tag{17}$$

where the integration is over the boundary surface of the structure, and

$$\mathbf{F}_i(t) = \begin{Bmatrix} F_i^x(t) \\ F_i^y(t) \\ F_i^z(t) \end{Bmatrix} \tag{18}$$

represents the nodal load on node i.

Using Eq.(16) and (17) the nodal loads are expressed as

$$\mathbf{F}_i(t) = \sum_{e_i} \int_{S_{e_i}} N_i^{e_i} \mathbf{I}\ \mathbf{p}(\mathbf{r},t) dS \quad , \tag{19}$$

where the summation is extended over all elements adjacent to node i, and the integration is over the boundary surface of each of these elements.

NODAL LOAD CORRELATION

Using Eq.(13) and (19) we obtain for the nodal load correlation

$$\mathbf{R}_{\mathbf{F}_i\mathbf{F}_j}(\tau) = \tag{20}$$

$$= \sum_{e_i} \sum_{e_j} \int_{S_{e_i}} \int_{S_{e_j}} N_i^{e_i} N_j^{e_j}\ \mathbf{R}_p(\mathbf{r}_{e_i},\mathbf{r}_{e_j},\tau) dS_{e_i} dS_{e_j},$$

where $\sum_{e_i}$ and $\sum_{e_j}$ are summations over elements adjacent to nodes i and j; and $\mathbf{r}_{e_i}$, $\mathbf{r}_{e_j}$ are distances to points on the boundary surface of these elements over which the integrations are extendent.

From Eq.(20) the nodal load cross-spectral matrix is obtained

$$\mathbf{S}_{\mathbf{F}_i\mathbf{F}_j}(\omega) = \tag{21}$$

$$= \sum_{e_i} \sum_{e_j} \int_{S_{e_i}} \int_{S_{e_j}} N_i^{e_i} N_j^{e_j}\ \mathbf{S}_p(\mathbf{r}_{e_i},\mathbf{r}_{e_j},\omega) dS_{e_i} dS_{e_j}.$$

Using Eq.(15) and (21) the nodal load cross-spectral amplitude matrix takes the form

$$|S_{F_i F_j}(\omega)| = \rho_{ij}(\omega)\, S_W(\omega) \quad , \tag{22}$$

where

$$\rho_{ij}(\omega) = \sum_{e_i} \sum_{e_j} \int_{S_{e_i}} \int_{S_{e_j}} N_i^{e_i} N_j^{e_j} \mathbf{H}(r_1)\mathbf{H}^{T}(r_2)\, \gamma(\Delta u, \omega)\, dS_{e_i} dS_{e_j} \; . \tag{23}$$

In global form Eq.(22) becomes

$$|\bar{S}_F(\omega)| = \bar{\rho}(\omega)\; S_W(\omega) \quad , \tag{24}$$

where $|\bar{S}_F(\omega)|$ is the global form of the nodal load cross-spectral amplitude matrix; and $\bar{\rho}(\omega)$ is the global form of $\rho_{ij}(\omega)$ matrix.

MONTE CARLO SIMULATION OF NODAL LOADS

In order to simulate the structural response in a short-crested sea a set of nodal forces are simulated with the help of N uncorrelated load series

$$X_1(t), X_2(t), \ldots, X_N(t) \quad , \tag{25}$$

where

$$X_i(t) = \begin{Bmatrix} X_i^x(t) \\ X_i^y(t) \\ X_i^z(t) \end{Bmatrix} \quad . \tag{26}$$

The number N of the load series is less or equal to the loaded nodal points on the boundary surface of the structure. Linear filtering methods (8) can be used to obtain the above series which satisfy

$$|S_{X_i X_j}(\omega)| = \begin{cases} I\, S_W(\omega) & \text{for } i=j \\ 0 & \text{for } i \neq j \end{cases} \quad , \tag{27}$$

where I is a (3*3) unit matrix.

The nodal loads are obtained from the load series $X_i(t)$ as

$$F_i(t) = \sum_{j=1}^{N} a_{ij}\, X_j(t) \quad , \tag{28}$$

or in global form

$$\bar{F}(t) = \bar{a}\; \bar{X}(t) \quad , \tag{29}$$

where $\bar{a}$ is the global form of a_{ij} matrix,

$$a_{ij} = \begin{bmatrix} a_{ij}^{xx} & a_{ij}^{xy} & a_{ij}^{xz} \\ a_{ij}^{yx} & a_{ij}^{yy} & a_{ij}^{yz} \\ a_{ij}^{zx} & a_{ij}^{zy} & a_{ij}^{zz} \end{bmatrix} \quad , \tag{30a}$$

and

$$\bar{X}(t) = \begin{Bmatrix} X_1(t) \\ X_2(t) \\ \vdots \\ X_N(t) \end{Bmatrix} \quad . \tag{30b}$$

From Eq.(29) and (27) we obtain

$$|\bar{S}_F(\omega)| = \bar{a}\; \bar{a}^{T}\, S_W(\omega) \quad . \tag{31}$$

For the time domain analysis assuming a narrow-banded wave loading, there is small variation of $\bar{\rho}(\omega)$ in the range of interesting frequencies, and from Eq.(24) and (31) we get

$$\bar{a}\; \bar{a}^{T} = \bar{\rho} \quad , \tag{32}$$

where $\bar{\rho}$ is the $\bar{\rho}(\omega)$ matrix evaluated for the mean wave frequency. The matrix $\bar{a}$ can be computed from Eq.(32) using the eigenvalue matrix Λ and the N eigenvectors Φ in respect to a unit matrix as

$$\bar{a} = \Phi\, \Lambda^{\frac{1}{2}}\, \Phi^{T} \quad . \tag{33}$$

After the simulation of the nodal loads the solution of the dynamic equations of motion proceeds in the usual deterministic way.

For the frequency domain analysis the frequency components of the force series $X_i(t)$ should be considered

$$X_i(t) = \sum_{k=1}^{M} c_i^k \cos(\omega_k t + \theta_i^k) \quad , \tag{34}$$

where c_i^k are amplitudes evaluated from the wave spectra , and θ_i^k are random phase angles between 0 and 2π . The nodal loads are obtained using Eq.(29)

$$\bar{F}(t) = \sum_{k=1}^{M} \bar{a}\; \bar{c}^k \cos(\omega_k t + \bar{\theta}^k) \quad , \tag{35}$$

where $\bar{c}^k$ and $\bar{\theta}^k$ are the global forms of c_i^k and θ_i^k matrices. The response to the harmonic loading of Eq.(35) is calculated for the further frequency domain analysis (10,12).

For the frequency domain analysis the narrow-banded assumption for the wave loading is not necessary. In this case the hydrodynamic transfer function $H(r,\omega)$ and the matrix $\bar{\rho}(\omega)$ are frequency dependent. The matrix $\bar{a}$ in Eq.(32) and (35) is also frequency dependent, and Eq.(33) must be used for each frequency ω_k.

To obtain the expected response values, a number of sea states are simulated by choosing different sets of the series $X_i(t)$. The expected response values are obtained from ensemble statistics between the simulated response values. The number of simulations is important in the accuracy of the final results. The optimum number of simulations can be obtained looking at the improvement in the accuracy of the resulting expected values as the number of simulations increases.

APPLICATION I, STEEL JACKET PLATFORMS

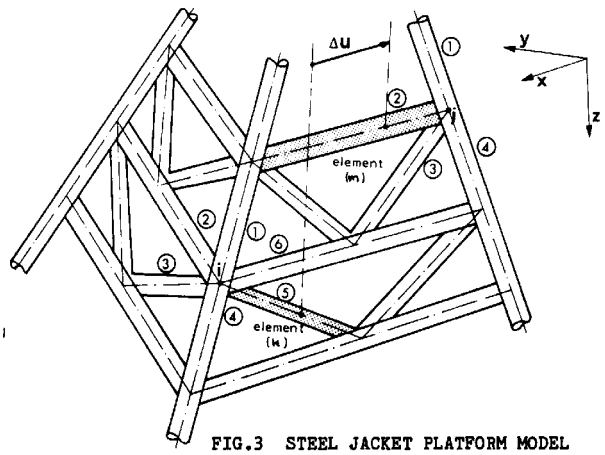

FIG.3 STEEL JACKET PLATFORM MODEL

Figure (3) shows a part of a model of steel jacket offshore platform. Applying Eq.(23) for the nodal points i and j we obtain

$$\rho_{ij}(\omega) = \sum_{k=1}^{6}\sum_{m=1}^{6} \int_{\ell_k}\int_{\ell_m} N_i^k N_j^m \, \mathbf{H}(r_1)\,\mathbf{H}^T(r_2)\,\gamma(\Delta u,\omega)\,d\ell_k d\ell_m \quad (36)$$

The hydrodynamic coefficients in the hydrodynamic transfer function $\mathbf{H}(r)$ are computed using Morison's equation and Eq.(10) and (12). If the coefficients are considered constant along each element, then Eq.(36) is simlified to the following

$$\rho_{ij}(\omega) = \sum_{k=1}^{6}\sum_{m=1}^{6} \mathbf{H}^k \mathbf{H}^{Tm} \int_{\ell_k}\int_{\ell_m} N_i^k N_j^m \gamma(\Delta u,\omega)\,d\ell_k d\ell_m \quad . \quad (37)$$

The integrals in Eq.(36) and (37) can be computed easily using a Gaussian integration scheme over each element. N_i^k and N_j^m are displacement functions for the elements k and m adjacent to nodes i and j and for unit displacements at these nodes. The term, $\gamma(\Delta u,\omega)$ is the wave coherence between the projections on the free surface of two points of the elements k and m.

APPLICATION II, GRAVITY PLATFORMS

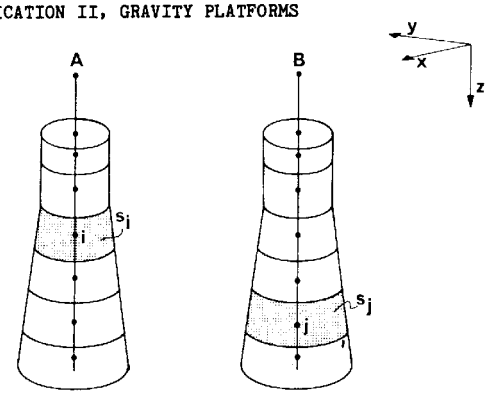

FIG.4 GRAVITY PLATFORM MODEL

Figure (4) shows a simplified model of a gravity platform. The legs have been subdivided into elements with the nodal points along the axis, where A, B are the points on the free surface. The hydrodynamic transfer functions $\mathbf{H}(r)$ are computed from the wave diffraction theory and Eq.(10) and (12). If we assume that the wave coherence does not vary significantly over the element size compared to the variation from one leg to the other, then Eq.(23) takes the simplified form

$$\rho_{ij}(\omega) = \gamma(\mathbf{u}_{AB},\omega) \int_{S_i} N_i \mathbf{H}(r_1)\,dS_i \int_{S_j} N_j \mathbf{H}^T(r_2)\,dS_j \quad , \quad (38)$$

or, alternately,

$$\rho_{ij}(\omega) = \mathbf{B}_i\, \gamma_{AB}(\omega)\, \mathbf{B}_j^T \quad , \quad (39)$$

where

$$\mathbf{B}_i = \int_{S_i} N_i \mathbf{H}(r)\, dS_i \quad , \quad (39a)$$

and $\gamma_{AB}(\omega)$ is the wave coherence between points A and B of the free surface. This means that the x,y,z components of the nodal loads at a node are fully correlated. In addition from Eq.(39), we can conclude that loads on the same leg are fully correlated. Then the simulation take a special form. Instead of the series of Eq.(25), we use the load series $X_1(t), X_2(t), \ldots, X_N(t)$, where N is the number of legs, and the nodal loads are obtained as

$$\mathbf{F}_i(t) = \mathbf{B}_i \sum_{j=1,N} a_{ij}\, X_j(t) \quad , \quad (40)$$

where the a_{ij} values are obtained from

$$\bar{\mathbf{a}}\,\bar{\mathbf{a}}^T = \bar{\bar{\gamma}} \quad . \quad (41)$$

Eq.(41) is similar to Eq.(32), but reduced in size by a considerable factor as the size of matrix $\bar{\bar{\gamma}}$, which is the global form of $\gamma_{AB}(\omega)$, is N^2, where N is the number of legs of the platform.

APPLICATION III, LONG FLOATING STRUCTURES

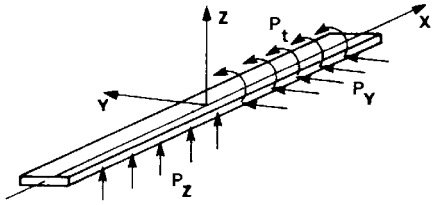

FIG.5 CONTINUOUS LONG FLOATING STRUCTURE

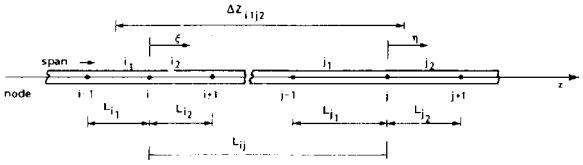

FIG.6 LONG FLOATING STRUCTURE MODEL

Figure (5) and (6) show a model of a long floating structure, like a floating bridge or a floating breakwater. The model is composed of beam elements. The components of the wave forces are the distributed forces p_y and p_z in the y and z direction and the moment around the x axis. The hydrodynamic transfer function is constant over the length of the structure, and it is computed using diffraction theory and Eq.(10) and (12) for the directional wave effects. Ref.(15) presents graphs and tables for the hydrodynamic coefficients in the case of long floating structures. Using the notation of Fig.(6), Eq.(23) becomes (10,11)

$$\rho_{ij}(\omega) = \mathbf{H}\,\mathbf{H}^T \rho^*_{ij}(\omega) \quad , \quad (42)$$

where

$$\rho^*_{ij}(\omega) = \quad (43)$$

$$= \sum_{k=1,2}\sum_{l=1,2} L_{i_k} L_{j_l} \int_0^1\int_0^1 N_{i_k}(\xi) N_{j_l}(\eta)\, \gamma\left(\frac{\Delta z_{i_k j_l}}{\lambda}\right) d\xi\, d\eta .$$

For Eq.(43) the notation of Fig.(6) is used, i_1 and i_2 are the spans left and right of the node i, j_1 and j_2 are the spans left and right of node j, ξ and η are

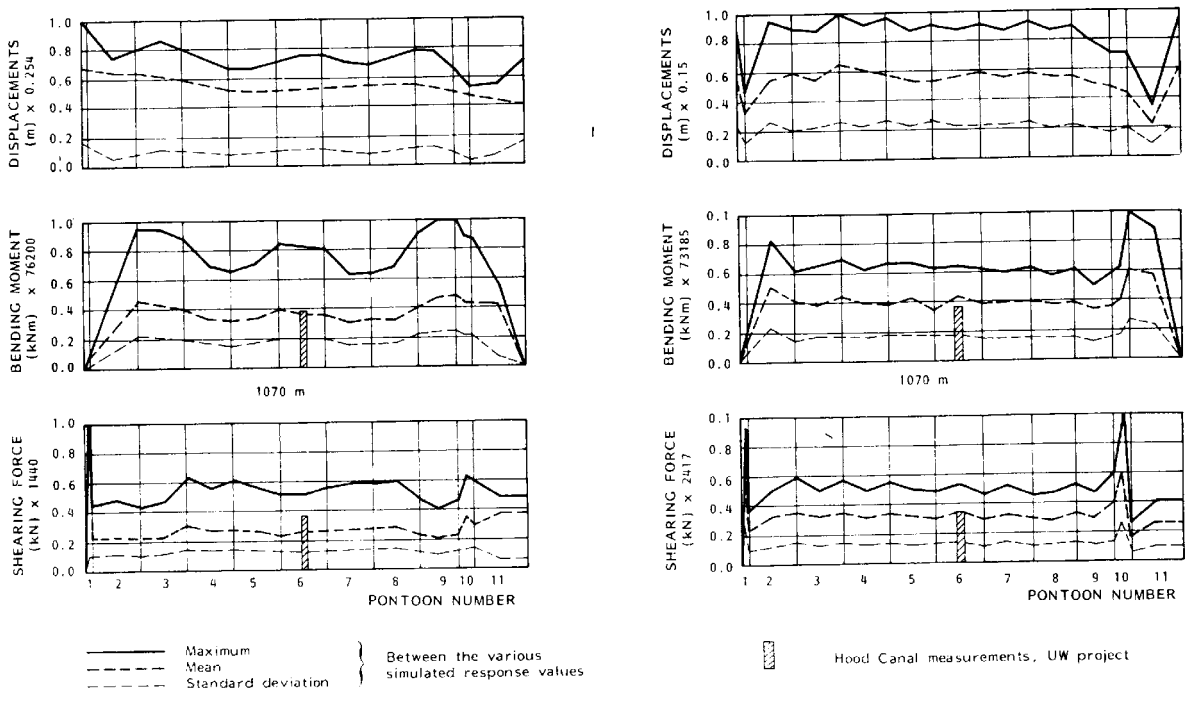

(A) Sway motion (B) Heave motion

FIG.7 SIMULATED RESPONSE OF THE ORIGINAL HOOD CANAL BRIDGE TO A MEASURED WAVE SPECTRUM

normal coordinates corresponding to spans adjacent to nodes i and j , $\Delta z_{i_k j_l}$ is the distance from a point in span i_k to a point in span j_1 , $N_{i_k}(\xi)$ and $N_{j_l}(\eta)$ are displacement functions for spans i_k and j_1 .

Again the special form of Eq.(39), makes the simulation easier since the three components of the nodal loads are correlated at each node. From the set of uncorrelated series $X_1(t), X_2(t), \ldots, X_N(t)$, where N is less than or equal to the loaded points, the nodal loads are obtained as

$$\mathbf{F}_i(t) = \mathbf{H}_i \sum_{j=1,N} a_{ij} X_j(t) \quad , \tag{44}$$

and the $\bar{\mathbf{a}}$ matrix

$$\bar{\mathbf{a}}\ \bar{\mathbf{a}}^T = \bar{\boldsymbol{\rho}}^* \quad , \tag{45}$$

where $\bar{\boldsymbol{\rho}}^*$ is the global form of the $\rho^*_{ij}(\omega)$ matrix. Equation (45) is similar to equation (32) but reduced in size by a factor of 3, because of the correlated components of the nodal forces.

NUMERICAL APPLICATION

An example of using the method, which has been presented, is shown in Fig.(7a and b), for the Hood Canal floating bridge. The total length of the modeled bridge is 1070 meters. The standard individual pontoons are closed, compartmented, reinforced prestressed, concrete units 16 meters wide, 4.5 meters deep and 120 meters long. The bridge is anchored laterally with long pretensioned cables every 120 meters perpendicular to the bridge axis and at an angle of 15° from the horizontal. More information about the bridge the wave loading on the bridge and the modeling methods, can be found in ref.(10),(11),(12), and (17). In Fig.(7a and b) are shown some results of the simulated response to a measured wave spectrum for the sway and heave motion. A directional wave spectrum model has been used with a spreading function of the cosine type and of a power 2.

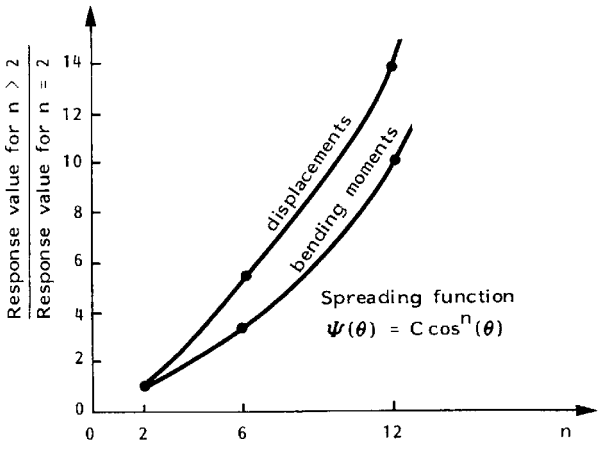

FIG.8 RESPONSE OF A FLOATING BREAKWATER TO THREE KINDS OF SHORT-CRESTED WAVE FIELD.

The wave coherence along the bridge is expressed as

$$\gamma(\Delta x/\lambda) = \exp(-8(|\Delta x|/\lambda)) \quad (46)$$

This agrees with in-situ measurments of wave pressure correlation along the bridge. Ensemble average maximum and standard deviation values for the response are shown in the figures, and as can be seen the ensemble average values approximate very closely the in-situ measurments for the same storm, at the center of the 6th pontoon, for both sway and heave response.

The importance of the short-crestness of the wave field in the response calculations can be seen from the results of Fig.(8) for the case of a floating breakwater. The response is simulated for three different kinds of short-crested seas corresponding to spreading functions of the cosine type with n=2,6,and 12. The results are normalized to the response values with n=2.

CONCLUSIONS

The work presented here deals with the evaluation of the response of structures under short-crested wave loading. The presented method can be applied to offshore platforms or floating bridges and breakwaters. The differences from the conventional methods are that it is based on a simulation process and it introduces the short-crested sea state directly in the response calculations without assuming superposition of directional components. The analysis proceeds as a deterministic dynamic analysis in time or frequency domain. The method can be easily implemented in a finite element program without extra memory requirements and long programming work (10,12).

A repetative solution is required to simulate the stochastic characteristics of the sea state. The expected response values are obtained from ensemble statistics between the results. Experience with long floating structures (10,11,12,17), which because of their length are the best example of structures in short-crested loading, showed satisfactory results with a number of simulations around 10.

For the load simulations an eigenvalue solution is required, Eq.(33), in order to obtain the nodal loads. The size of the matrices for eigenvalue solution is not large, as only the loaded degrees of freedom are considered. The number of obtained eigenvectors is not necessary large. As has been also shown in the case of gravity platforms, and long floating structures, the size of the matrices for the eigenvalue solution in the load simulation, is reduced considerably, due to the correlation of the nodal components or the correlation between the loads of certain nodal groups.

The method can be used for time domain analysis, under the assumption of narrow-banded loading, in order to use constant values for the hydrodynamic coefficients and the wave coherence. Since the simulation methods concerned only with the computation of nodal loads from the short-crested sea, the method can be used for nonlinear time domain dynamic analysis. The nonlinearites which can be introduced are due to either the structure, the foundation or the anchoring system.

REFERENCES

1 Sigbjornsson, R. "Stochastic Theory of Wave Loading Process," Engineering Structures, 1, 2, 1979, pp.58-64.

2 Garrison, C.J. "Hydrodynamic Loading of Large Offshore Structures; Three-dimensional Source Distribution Methods", Numerical Methods in Offshore Engineering, John Wiley, New York 1978, pp87-140.

3 Sigbjornsson, R., Bell, K., Holland,I. "Dynamic Response of Framed and Gravity Structures to Waves", Numerical Methods in Offshore Engineering, John Wiley, New York 1978, pp245-280.

4 Kinsman, B. "Wind Waves, their Generation and Propagation on the Ocean Surface", Prentice Hall, 1965.

5 Borgman, L.E. " The Estimation of Parameters in a Circular Normal Two-Dimensional Wave Spectrum", Techn. Report HEL 1-9, Hydraulic Engineering Laboratory, University of California, Berkeley, 1967.

6 Panicker, N.N. "Review of Techniques for Directional Spectra", Proc. Int. Symp. on Ocean Wave Measurment and Analysis", ASCE, vol. 1, 1974.

7 Madria,K.V. "Statistics of Directional Data," Academic Press, 1972.

8 Borgman, L.E. "Ocean Wave Simulation for Engineering Design", J. ASCE WW4, Vol.95, 1969, pp556-583.

9 Georgiadis,C. and Hartz,B.J. " Wave Coherence Along Continuous Floating Structures for Directional Spectral Models," Report, SINTEF, STF71-A82004, Trondheim, Norway, 1982.

10 Georgiadis, C. "Wave Induced Vibrations in Continuous Floating Structures", Ph.D. dissertation, University of Washington, Seattle, 1981.

11 Hartz, B.J., Georgiadis, C. "A Finite element Program for the dynamic Response of continuous Floating Structures in Short-Crested Waves", International Conference on Finite Element Methods, Shanghai China 1981, pp493-498.

12 Georgiadis, C., Hartz, B.J. "Theory and Experiment for the Response of Long Floating Structures", 4th International Symposium on Offshore Engineering, Rio de Janeiro, Brazil, Sept. 1983.

13 Brebbia, C.A. and Walker,S. "Dynamic Analysis of Offshore Structures", Newnes-Butterworths, London, 1979.

14 Georgiadis, C., Hartz, B.J."A Boundary Element Program for the Computation of the Three-dimensional Hydrodynamic Coefficients", International Conference on Finite Element Methods, Shanghai China 1981, pp487-492.

15 Georgiadis, C. "Hydrodynamic Forces on Long Floating Structures in Directional Wave Fields," Report, SINTEF, STF71-A83007, Trondheim, Norway, 1983.

16 Zienkiewicz,O.C."The Finite Element Method," Third Edition, Mc.Graw-Hill, London,1977.

17 Hartz, B.J. " Dynamic Analysis of the Hood Canal Floating Bridge Failure" Proc. 3rd International Conference on Structural Safety and Reliability, Trondheim, Norway 1981.

reprinted from

Proceedings of the Third International Offshore Mechanics and Arctic Engineering Symposium – Volume I
Editor: Jin S. Chung
(Book No. I00171)

published by

THE AMERICAN SOCIETY OF MECHANICAL ENGINEERS
345 East 47th Street, New York, N.Y. 10017
Printed in U.S.A.